Journal of Power Sources 195 (2010) 4410–4413

Contents lists available at ScienceDirect

Journal of Power Sources

journal homepage: www.elsevier.com/locate/jpowsour

Short communication

MnO_2 nanotube and nanowire arrays by electrochemical deposition for supercapacitors

Hui Xia, Jinkui Feng, Hailong Wang, Man On Lai, Li Lu*

Department of Mechanical Engineering, National University of Singapore, 9 Engineering Drive 1, Singapore 117576, Singapore

ARTICLE INFO

Article history:
Received 17 December 2009
Received in revised form
30 December 2009
Accepted 20 January 2010
Available online 4 February 2010

Keywords:
Supercapacitor
Manganese dioxide
Nanotube array
Nanowire array
Cyclic voltammetry

ABSTRACT

Highly ordered MnO_2 nanotube and nanowire arrays are successfully synthesized via a electrochemical deposition technique using porous alumina templates. The morphologies and microstructures of the MnO_2 nanotube and nanowire arrays are investigated by field emission scanning electron microscopy and transmission electron microscopy. Electrochemical characterization demonstrates that the MnO_2 nanotube array electrode has superior capacitive behaviour to that of the MnO_2 nanowire array electrode. In addition to high specific capacitance, the MnO_2 nanotube array electrode also exhibits good rate capability and good cycling stability, which makes it promising candidate for supercapacitors.

1. Introduction

As alternative energy storage devices, supercapacitors have gained increasing attention due to their higher specific power and long cycle life compared with rechargeable batteries, and higher specific energy compared with conventional capacitors [1]. Active electrode materials used in supercapacitors can be classified into three main categories: carbon, conducting polymer, and transition metal oxide. In particular, ruthenium oxide (RuO_2) is considered as the most promising material as it offers high specific capacitance with excellent cycling stability [2]. On the other hand, the high cost and toxicity of RuO_2 limits its commercial application. Therefore, intensive studies have been carried out to find alternative, inexpensive electrode materials. One candidate is manganese dioxide (MnO_2) that has been extensively investigated with the anticipation that MnO_2 will replace RuO_2 as a low-cost and 'green' electrode material [3–5].

To develop high performance supercapacitors, electrode materials with three-dimensional (3D), mesoporous and ordered/aperiodic architectures are desirable for the penetration of electrolyte and reactants into the whole electrode matrix [2]. To prepare composite electrodes for supercapacitors, electronic conductors and binders are often mixed with the electrode materials. This, however, not only reduces the specific energy of the devices but also adds an extra contact resistance between the current-collectors and the electrode materials. Significant improvements in supercapacitor performance have been obtained by using ordered active nanostructures grown directly on current-collector substrates [2,6,7]. Although various nanostructures of MnO_2, such as nanoflake, nanowire and nanotube, have been fabricated, it is still a challenge to prepare highly ordered arrays of such nanostructures directly on metal substrates. To date, only a few reports have been published on the synthesis of MnO_2 nanowire or nanotube arrays on metal substrates [8–10].

Previous investigations of the electrochemical deposition of MnO_2 electrodes using alumina membranes have only revealed the morphology of nanowire arrays [8,9]. Herein, MnO_2 nanotube arrays are synthesized by electrochemical deposition using porous alumina templates. It has been found that the MnO_2 nanotube arrays exhibit superior capacitive behaviour, thus making them promising as electrodes for supercapacitors.

2. Experimental

To prepare MnO_2 nanotube and nanowire arrays, an electrochemical deposition technique was used. A solution with 0.1 M manganese sulfate (Aldrich) and 0.1 M sodium sulfate (Aldrich) was used as the electrolyte. Alumina membranes of 200 nm in pore diameter and 60 μm in thickness were used as the templates (Whatman). To prepare the working electrode, a thin layer of platinum (Pt) was first sputtered on one side of the alumina membrane using a sputter coating system (JEOL JFC-1200). The

* Corresponding author. Tel.: +65 6516 2236; fax: +65 6779 1459.
E-mail address: luli@nus.edu.sg (L. Lu).

0378-7753/$ – see front matter © 2010 Elsevier B.V. All rights reserved.
doi:10.1016/j.jpowsour.2010.01.075

Pt-coated membrane was then pasted on a Pt substrate using Pt paste. After drying, the Pt substrate and alumina membrane was heated at 700 °C for 30 min to enhance the adhesion between the two components. Parafilm was used to cover the exposed area of the Pt substrate so that only the alumina template surface was exposed. The electrochemical cell consisted of a working electrode, a carbon rod counter electrode, and a Ag|AgCl (CHI111) reference electrode. Electrochemical deposition of MnO_2 was performed under galvanostatic conditions at a constant current of 2 mA cm^{-2}. The nanotube and nanowire morphologies were controlled by varying the deposition time. A period of 10 min was used for MnO_2 nanotube array synthesis, whereas 60 min was used for MnO_2 nanowire array synthesis. After electrochemical deposition, the samples were immersed in an 1 M KOH solution overnight to remove the alumina template. After being rinsed with de-ionized water repeatedly, the samples were dried in air for further characterization.

The morphologies and microstructures of as-prepared samples were characterized by means of a field emission scanning electron microscope (FESEM, Hitachi, S-4300) and a transmission electron microscope (TEM, JEOL 3010). Chemical-state analysis was carried out by X-ray photoelectron spectroscopy (XPS) using an Axis Ultra DLD XPS spectrometer. The weight of the active material was calculated from the charge passed for the electrochemical deposition (the calculation results agree well with weight measurements by a electronic balance with less than 5% difference). The supercapacitive properties of the as-prepared electrodes were investigated in a 1 M Na_2SO_4 electrolyte solution by cyclic voltammetry (CV) and galvanostatic charge–discharge cycling using a Solartron 1287 electrochemical interface. The electrochemical cell consisted of a working electrode (the as-prepared electrodes), a carbon rod counter electrode, and a Ag|AgCl reference electrode.

3. Results and discussion

Fig. 1 shows the FESEM images of MnO_2 nanotube arrays and MnO_2 nanowire arrays at different magnifications after removal of the template, namely: a top view of uniform MnO_2 nanotube arrays (Fig. 1(a)); the formation of the homogeneous nanotublar arrayed structure (Fig. 1(b)); cross-sectional view of MnO_2 nanotube arrays, from which the length of MnO_2 nanotube is estimated to be about 2 μm (Fig. 1(c)). With prolonged electrochemical deposition, the morphology of the nanotublar nanostructure changes to a wire-like form, as shown in Fig. 1(d) and (e). From a cross-sectional view of the MnO_2 nanowire arrays (Fig. 1(f)), the length of MnO_2 nanowire is estimated to be about 10 μm. It has been proposed [11] that the nanostructure generated in the process of electrochemical deposition of metal within an alumina template is controlled by the deposition conditions. The nanotube structure appears to originate from the shape of the plasma-deposited base electrodes, and this shape changes to the filled nanowire at an early stage of the electroplating process under normal, low-current-density conditions [11,12]. A similar phenomenon is observed for the electrochemical deposition of MnO_2 within a porous alumina template. The plasma-sputtered Pt on the bottom surface of the alumina template and a portion of the inside channel surface generate ring morphology and MnO_2 deposition starts to form a tube-like structure. As the deposition continues, the tube starts to be filled. Deposition for a very long time, such as 60 min, finally leads to wire-like MnO_2 arrays. Therefore, it is important to pay attention to the deposition time when preparing tubular oxides by means of electrochemical deposition with templates.

To understand the structure in further detail, the MnO_2 nanotubes and nanowires were investigated with TEM. An image of an open-ended MnO_2 tube at low magnification is given in Fig. 2(a). The centre of the tubular structure is bright in contrast to its edges, thereby confirming its hollow-tube nature. The electron diffraction pattern (ED) given in the insert of Fig. 2(a) reveals that the electrodeposited MnO_2 tube is amorphous, which is further confirmed by X-ray diffraction analysis (result not shown here). As shown in Fig. 2(b), the inner diameter of the tube is about 120–130 nm, and the wall thickness is about 40–50 nm. A TEM image of a broken MnO_2 nanowire at low magnification is presented in Fig. 2(c); the insert shows that the electrodeposited MnO_2 nanowire is also amorphous, which agrees with TEM analysis of the MnO_2 nanotube. As shown in Fig. 2(d), the diameter of the nanowire is about 200 nm, which corresponds to the diameter of the alumina template used.

The Mn 2p and O 1s XPS spectra of the MnO_2 nanotube arrays are given in Fig. 3. As shown in the Mn 2p spectrum, two peaks located at 642.1 and 653.7 eV can be attributed to Mn 2p3/2 and Mn 2p1/2, respectively. The peak values agree well with those reported

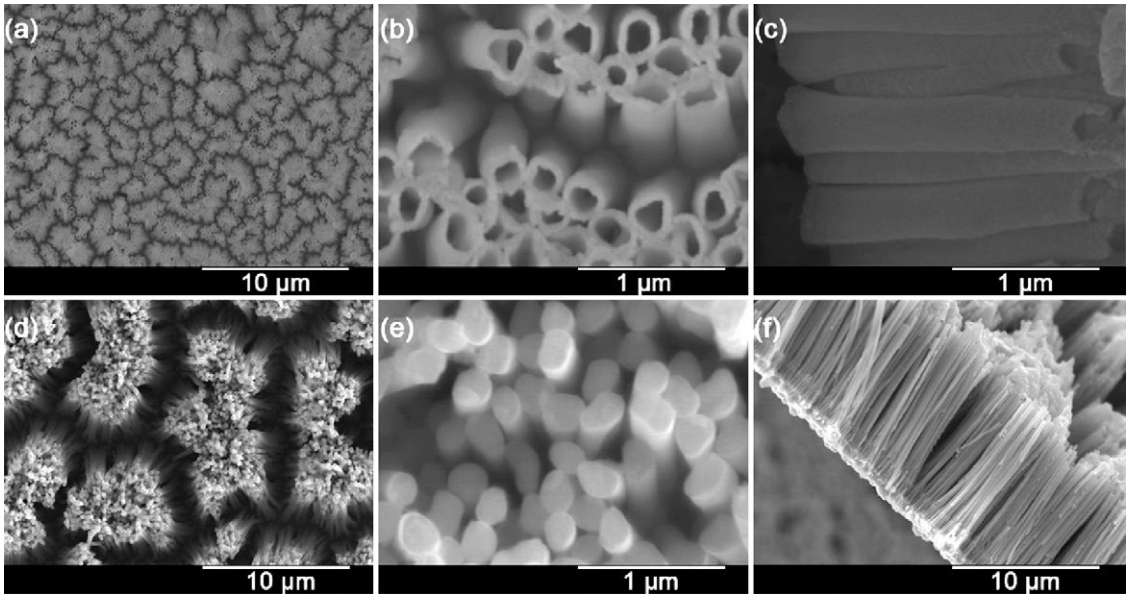

Fig. 1. (a) and (b) top view FESEM images of MnO_2 nanotube arrays; (c) cross-sectional FESEM image of MnO_2 nanotube arrays; (d) and (e) top view FESEM images of MnO_2 nanowire arrays; (f) cross-sectional FESEM image of MnO_2 nanowire arrays.

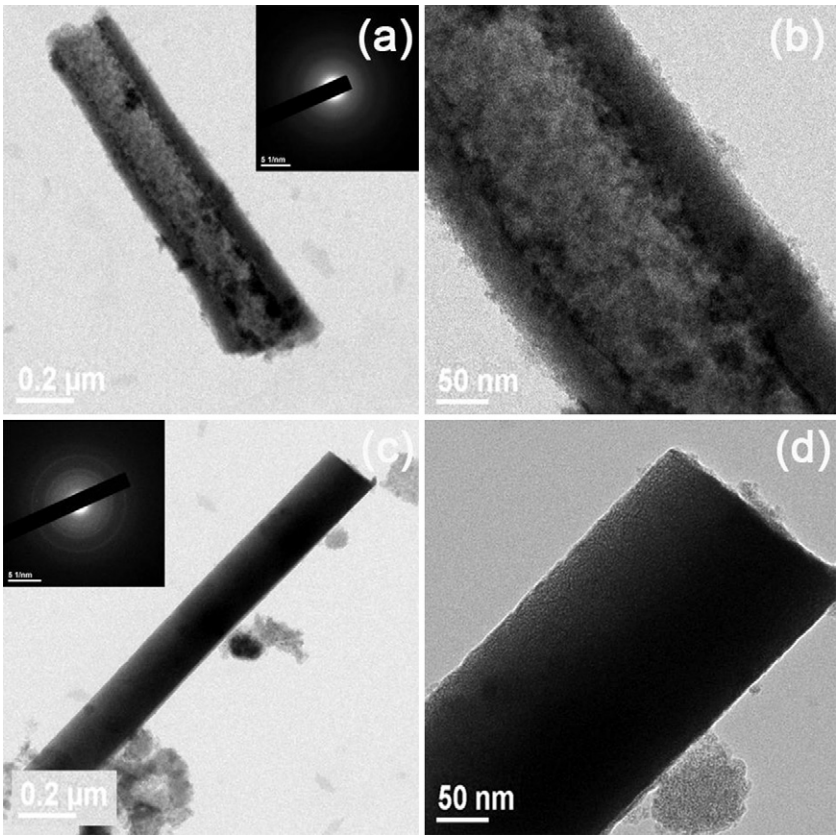

Fig. 2. (a) and (b) TEM images of open-ended MnO_2 nanotube (inset in (a) shows corresponding ED pattern); (c) and (d) TEM images of broken MnO_2 nanowire (inset in (c) shows corresponding ED pattern).

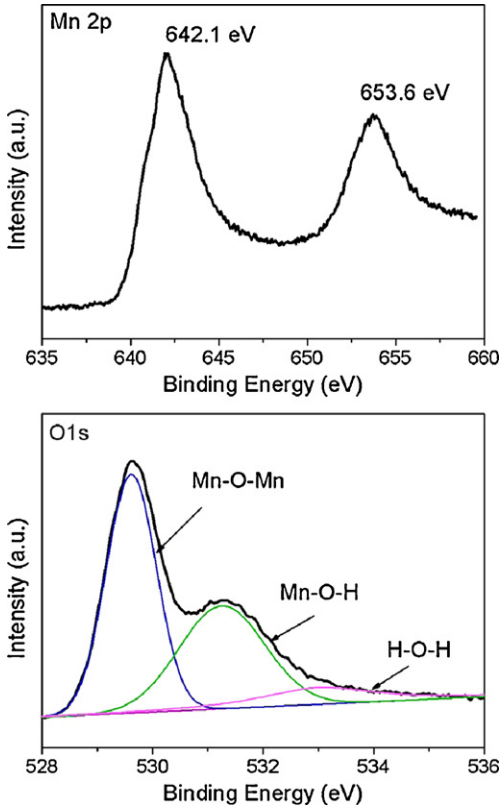

Fig. 3. (a) Mn 2P XPS spectrum and (b) O 1s XPS spectrum for MnO_2 nanotube arrays.

for MnO_2 and indicate a 4+ oxidation state for Mn [13,14]. The O 1s spectrum can be deconvoluted into three components that correspond to three different types of oxygen bonds: Mn–O–Mn, Mn–O–H, and H–O–H [13]. The XPS results are in good agreement with those obtained by other workers for electrodeposited MnO_2 thin films [13,14]. Quantitative XPS analysis indicates that the atomic ratio of Mn to O is approximately 0.5, thereby confirming the MnO_2 composition.

To investigate the electrochemical properties of the as-prepared MnO_2 nanotube and nanowire array electrodes, CV measurements were conducted in 1 M Na_2SO_4 electrolyte. Fig. 4(a) and (b) shows typical CV curves between 0 and 1.0 V at a scan rate of 20 mV s^{-1} for the MnO_2 nanotube array electrode and the MnO_2 nanowire array electrode, respectively. The CV curves for the nanotube array are close to a rectangular shape and exhibit a mirror-image feature, thus demonstrating the good reversibility and ideal capacitive properties of the electrode. By contrast, obvious distortion from the rectangular shape in the CV curves in Fig. 4b indicates the poor capacitive properties of the MnO_2 nanowire array electrode. The specific capacitances for the MnO_2 nanotube and nanowire array electrodes are calculated to be 320 and 101 F g^{-1}, respectively. The superior capacitive behaviour of the MnO_2 nanotube array can be attributed to its nanotubular architecture, which provides much shorter diffusion paths for both cations and electrons. Galvanostatic charge–discharge curves for the MnO_2 nanotube array electrode measured between 0 and 1.0 V at different current densities are presented in Fig. 4(c). The average specific capacitances are calculated to be 349, 325, 285, and 245 F g^{-1} for current densities of 1, 2, 5, and 10 A g^{-1}, respectively. Around 70% initial capacitance retention can be retained even when the current density increases by as much as ten times, thus indicating good rate capability. The cycle performance of the MnO_2 nanotube array electrode is shown

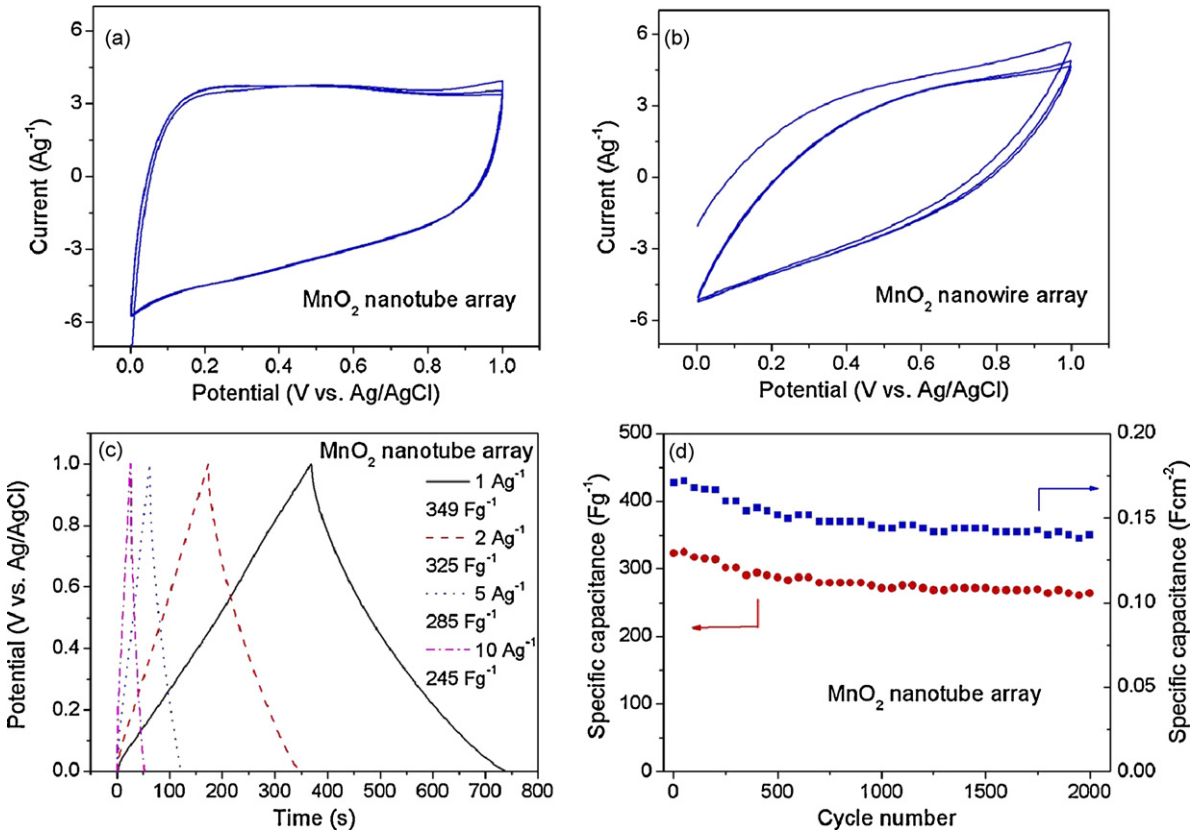

Fig. 4. (a) CV curves of MnO_2 nanotube array electrode at scan rate of 20 mV s^{-1}; (b) CV curves of MnO_2 nanowire array electrode at scan rate of 20 mV s^{-1}; (c) charge–discharge curves of MnO_2 nanotube array electrode at different current densities; (d) mass-specific capacitance and area-specific capacitance as function of cycle number.

in Fig. 4(d). About 81% of its initial capacitance is retained after 2000 cycles, again indicating good cycling stability. In addition to the mass-specific capacitance ($F g^{-1}$), the area-specific capacitance ($F cm^{-2}$) is also important for practical applications. As shown in Fig. 4(d), the MnO_2 nanotube array electrode can have a relatively high area-specific capacitance of 0.15 $F cm^{-2}$ while keeping a high mass-specific capacitance of 320 $F g^{-1}$.

4. Conclusions

For the first time, free-standing MnO_2 nanotube arrays on a Pt substrate have been synthesized by an electrochemical deposition technique that employs porous alumina templates. By increasing the deposition time, the initial generated tubular morphology will transform to wire-like morphology. The MnO_2 nanotube array electrode exhibits superior capacitive behaviour to that of the MnO_2 nanowire array electrode. This feature can be attributed to the unique nanotubular architecture of the former electrode that offers fast ion and electron transport. With both high mass-specific capacitance and high area-specific capacitance, MnO_2 nanotube array electrodes are promising candidates for supercapacitors.

Acknowledgements

The research was supported by the National University of Singapore and the Agency for Science, Technology and Research through research grant R-284-000-067-597 (072 133 0044).

References

[1] P. Simon, Y. Gogotsi, Nat. Mater. 7 (2008) 845.
[2] C.C. Hu, K.H. Chang, M.C. Lin, Y.T. Wu, Nano Lett. 6 (2006) 2690.
[3] S.L. Chou, J.Z. Wang, S.Y. Chew, H.K. Liu, S.X. Dou, Electrochem. Commun. 10 (2008) 1724.
[4] S.L. Chou, F.Y. Cheng, J. Chen, J. Power Sources 162 (2006) 727.
[5] H. Xia, W. Xiao, M.O. Lai, L. Lu, Nanoscale Res. Lett. 4 (2009) 1035.
[6] H. Zhang, G.P. Cao, Z.Y. Wang, Y.S. Yang, Z.J. Shi, Z.N. Gu, Nano Lett. 8 (2008) 2664.
[7] S. Lee, M.S. Cho, J.D. Nam, Y. Lee, J. Nanosci. Nanotechnol. 8 (2008) 5036.
[8] R. Liu, S.B. Lee, J. Am. Chem. Soc. 130 (2008) 2942.
[9] C.L. Xu, S.J. Bao, L.B. Kong, H. Li, H.L. Li, J. Solid State Chem. 179 (2006) 1351.
[10] A.L.M. Reddy, M.M. Shaijumon, S.R. Gowda, P.M. Ajayan, Nano Lett. 9 (2009) 1002.
[11] W.C. Yoo, J.K. Lee, Adv. Mater. 16 (2004) 1097.
[12] S.L. Chou, F.Y. Cheng, J. Chen, Eur. J. Inorg. Chem. (2005) 4035.
[13] W.F. Wei, X.W. Cui, W.X. Chen, D.G. Ivey, J. Phys. Chem. C 112 (2008) 15075.
[14] W. Xiao, H. Xia, J.Y.H. Fuh, L. Lu, J. Electrochem. Soc. 156 (2009) A627.